OPEN ACCESS

Coherent oscillations in a superconducting tunable flux qubit manipulated without microwaves

New Journal of Physics
The open-access journal for physics

Coherent oscillations in a superconducting tunable flux qubit manipulated without microwaves

S Poletto[1], F Chiarello[2], M G Castellano[2], J Lisenfeld[1], A Lukashenko[1], C Cosmelli[3], G Torrioli[2], P Carelli[4] and A V Ustinov[1,5]

[1] Physikalisches Institut, Universität Karlsruhe (TH), D-76131 Karlsruhe, Germany
[2] Istituto di Fotonica e Nanotecnologie, CNR, 00156 Roma, Italy
[3] Dipartimento Fisica, Università di Roma La Sapienza, 00185 Roma, Italy
[4] Dipartimento Ingegneria Elettrica, Università dell'Aquila, 67040 Monteluco di Roio, Italy
E-mail: ustinov@physik.uni-karlsruhe.de

New Journal of Physics **11** (2009) 013009 (10pp)
Received 10 September 2008
Published 7 January 2009
Online at http://www.njp.org/
doi:10.1088/1367-2630/11/1/013009

Abstract. We experimentally demonstrate coherent oscillations of a tunable superconducting flux qubit by manipulating its energy potential with a nanosecond-long pulse of magnetic flux. The occupation probabilities of two persistent current states oscillate at a frequency ranging from 6 GHz to 21 GHz, tunable by changing the amplitude of the flux pulse. The demonstrated operation mode could allow quantum gates to be realized in less than 100 ps, which is much shorter than gate times attainable in other superconducting qubits. Another advantage of this type of qubit is its immunity to both thermal and magnetic field fluctuations.

Superconducting qubits are among the most promising systems for the realization of quantum computation. Coherent quantum evolution and manipulation have been demonstrated and extensively studied for single [1]–[5] and coupled superconducting qubits [6]–[12]. In most cases, the state of superconducting qubits is controlled by resonant microwave pulses using a technique similar to the nuclear magnetic resonance (NMR) manipulation of atoms. As we show here, an alternative way to manipulate qubits is to modify their energy potential by means of fast (non-adiabatic) dc-pulses of magnetic bias flux [1, 5].

[5] Author to whom any correspondence should be addressed.

To date, extensive studies on superconducting flux [3], [13]–[15] and phase [16]–[19] qubits have shown that microwave-based qubit control may provide an excellent fidelity of logical gate operations. However, avoiding the necessity of microwave pulses for qubit control may greatly simplify the design of a scaled-up quantum processor which consists of many qubits. Spurious cross-talk of the high frequency signal between qubits is a problem that will become serious in a highly integrated quantum circuit. A further disadvantage is the relatively long duration of single qubit gates when realized by microwave pulses. In order to avoid population of higher excited qubit states, the Rabi oscillation frequency must be kept below a typical value of about 250 MHz, which is related to the anharmonicity of the potential well [20]–[22]. Therefore, the duration of a single-qubit NOT gate, which takes half the period of the Rabi oscillation, is practically longer than about 5 ns, whereas the longest coherence times obtained so far are below 2 μs [23, 24]. Knill [25] argued that at least 10^4 quantum gates are required during the coherence time in order to implement quantum error correction algorithms that are able to restore the loss of quantum information. To reach this limit with qubits controlled by microwaves, the only practicable way is increasing the coherence time.

In this paper, we report the observation of tunable coherent oscillations in a superconducting quantum interference device (SQUID)-based flux qubit which were obtained by manipulating the qubit with pulses of magnetic flux rather than microwaves. By this technique, we could increase the oscillation frequency up to 21 GHz, which allows very fast logical quantum gates to be performed. In addition, manipulating the qubit by modifying its energy potential profile requires a much simpler experimental technique and offers the possibility of using classical logic signals to control a quantum processor, which is advantageous for the large scale implementation of quantum circuits.

The investigated circuit, shown in figure 1(a), is a double SQUID consisting of a superconducting loop of inductance $L = 85$ pH, interrupted by a small dc SQUID of loop inductance $l = 6$ pH. This dc SQUID is operated as a single Josephson junction (JJ) whose critical current is tunable by an external magnetic field. Each of the two JJs embedded in the dc SQUID has a critical current $I_0 = 8\,\mu$A and capacitance $C = 0.4$ pF. The qubit is manipulated by changing two magnetic fluxes Φ_x and Φ_c, applied to the large and small loops by means of two coils of mutual inductance $M_x = 2.6$ pH and $M_c = 6.3$ pH, respectively. Readout of the qubit flux is performed by measuring the switching current of an unshunted dc SQUID, which is inductively coupled to the qubit [26]. The circuit was manufactured by Hypres[6] using standard $Nb/AlO_x/Nb$ technology in a 100 A cm^{-2} critical current density process. The dielectric material used for junction isolation is SiO_2. The whole circuit is designed gradiometrically in order to reduce magnetic flux pick-up and spurious flux couplings between the loops. The JJs have dimensions of $3 \times 3\,\mu$m^2 and the entire device occupied a space of $230 \times 430\,\mu$m^2. All the measurements were performed at a sample temperature of 15 mK. The currents generating the two fluxes Φ_x and Φ_c were supplied via coaxial cables including 10 dB attenuators at the 1 K-pot stage of a dilution refrigerator. To generate the flux Φ_c, a bias-tee at room temperature was used to combine the outputs of a current source and a pulse generator. For biasing and sensing the readout dc SQUID, we used superconducting wires and metal powder filters [27] at the base temperature, as well as attenuators and low-pass filters with a cut-off frequency of 10 kHz at the 1 K-pot stage. The chip holder with the powder filters was surrounded by one superconducting and two cryoperm shields.

[6] Hypres Inc., Elmsford, NY, USA.

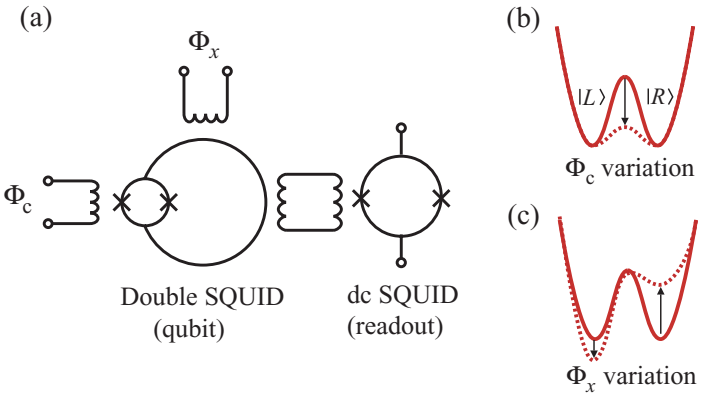

Figure 1. (a) Schematic of the flux qubit circuit. (b) The control flux Φ_c changes the potential barrier between the two flux states $|L\rangle$ and $|R\rangle$, here $\Phi_x = 0.5\,\Phi_0$. (c) Effect of the control flux Φ_x on the potential symmetry.

Assuming identical junctions and negligible inductance of the smaller loop ($l \ll L$), the system dynamics is equivalent to the motion of a particle with the Hamiltonian

$$H = \frac{p^2}{2M} + \frac{\Phi_b^2}{L}\left[\frac{1}{2}(\varphi - \varphi_x)^2 - \beta(\varphi_c)\cos\varphi\right],$$

where $\varphi = \Phi/\Phi_b$ is the spatial coordinate of the equivalent particle, p is the relative conjugate momentum, $M = C\Phi_b^2$ is the effective mass, $\varphi_x = \Phi_x/\Phi_b$ and $\varphi_c = \pi\ \Phi_c/\Phi_0$ are the normalized flux controls, and $\beta(\varphi_c) = (2I_0L/\Phi_b)\cos\varphi_c$, with $\Phi_0 = h/(2e)$ and $\Phi_b = \Phi_0/(2\pi)$. For $\beta < 1$ the potential has a single minimum, otherwise it consists of multiple wells. In the particular case of $1 < \beta < 4.6$ and $\Phi_x = \Phi_0/2$, the system potential is a symmetric double well shown in figure 1(b). The two states $|L\rangle$ and $|R\rangle$, which are, respectively, localized in the left and right potential well, correspond to a persistent current circulating either clockwise or counter-clockwise in the main SQUID loop. As shown in figure 1(b), the external flux Φ_c controls the height of the barrier separating the minima, whereas a variation of Φ_x changes the symmetry of the potential as indicated in figure 1(c). In this work, we exploit both the double well and the single well properties. The double well potential shape is used for qubit initialization and readout. The single well, or more exactly the two lowest energy states $|0\rangle$ and $|1\rangle$ in this well, is used for the coherent evolution of the qubit.

We use a well established procedure [28] to identify the regions where the system has a double well potential in the $\Phi_c - \Phi_x$ plane. The flux response Φ of the qubit is measured as a function of Φ_x and Φ_c fluxes and the switching points between different flux states are detected. Figure 2(a) shows $\Phi - \Phi_x$ characteristics obtained for two Φ_c values using initial state preparation in different wells. A region of bi-stability, indicating a double potential well, is observed in the vicinity of $\Phi_x \approx 0.5\Phi_0$, whereas outside of the hysteretic curve the potential has a single potential well. At the border between these regions we find abrupt switching between the two stable states. The positions Φ_x of the switching points are plotted in figure 2(b) for different Φ_c values. This diagram allows to easily identify the combinations of parameters resulting in a single- or double-well potential. A single-well region is found for $\Phi_c \gtrsim 0.42$ regardless of the chosen Φ_x value.

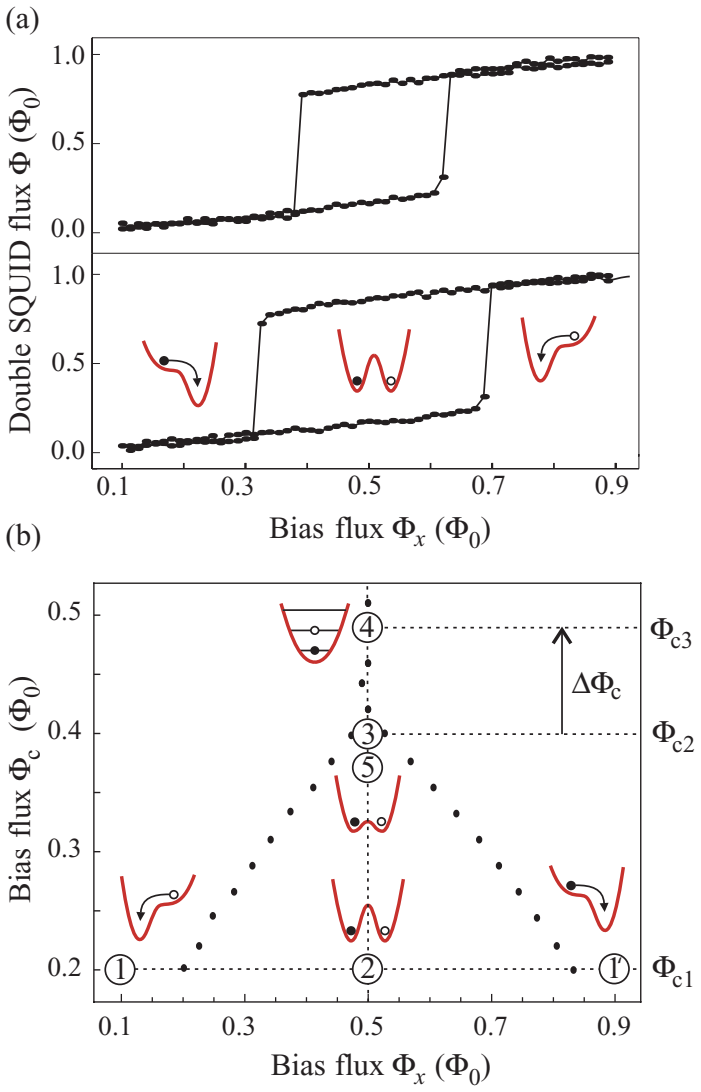

Figure 2. (a) The measured double SQUID flux Φ dependence on Φ_x, plotted for two different values of Φ_c and initial preparation in either potential well. (b) Position of the switching points (dots) in the $\Phi_c - \Phi_x$ parameter space. Numbered tags indicate the working points for qubit manipulation at which the qubit potential has a shape as indicated in the insets.

The measurement process that we used to observe coherent oscillations consists of several steps as shown in figure 3(a). Each step is realized by applying a combination of magnetic fluxes Φ_x and Φ_c as indicated by numbers in figure 2(b). The first step in our measurement is the initialization of the system in a defined flux state (1). Starting from a double well at $\Phi_x \cong \Phi_0/2$ with high barrier, the potential is tilted by changing Φ_x until it has only a single minimum (left or right, depending on the amplitude and polarity of the applied flux pulse). This potential shape is maintained long enough to ensure relaxation to the ground state. Afterwards, the potential is tuned back to the initial double-well state (2). The high barrier prevents any tunneling and the qubit is thus initialized in the chosen potential well. Next, the barrier height

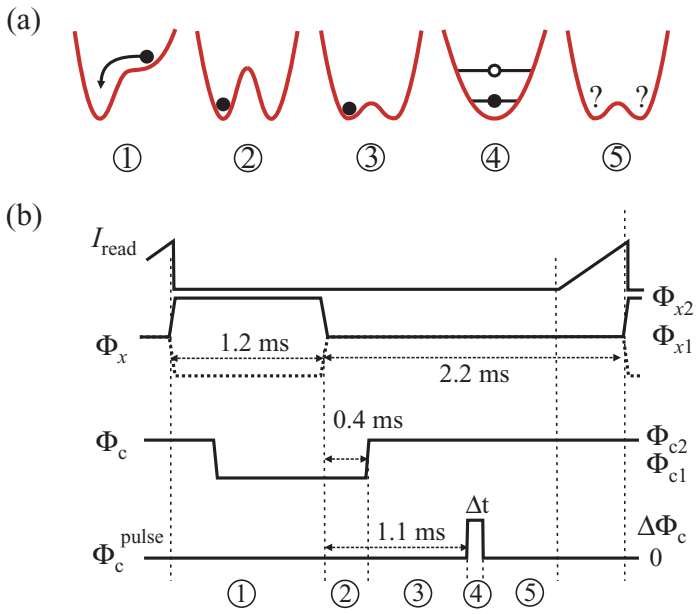

Figure 3. (a) Variation of the potential shape during the manipulation. (b) Time sequence of the readout dc SQUID current (topmost line) and flux bias values (bottom lines). The solid and dashed lines in the Φ_x curve correspond to initialization in opposite potential wells.

is lowered to an intermediate level (3) that preserves the initial state but allows just a small-amplitude Φ_c flux pulse to be used for the subsequent manipulation. The following Φ_c-pulse transforms the potential into a single well (4) for a duration Δt in the nanosecond range. In this situation, the relative phase of the ground and the first excited states evolves depending on the energy difference between them. After the end of the Φ_c-pulse, the double well is restored and the system is measured in the basis $\{|L\rangle, |R\rangle\}$ (5). The readout of the qubit flux state is accomplished by starting a bias current ramp to the dc SQUID and recording its switching current to the voltage state.

The pulse sequence that realizes the above described manipulation is reported in figure 3(b). The flux Φ_x is switched between two values: Φ_{x2} is used to create a strongly asymmetric potential for qubit initialization in the left or right well, and Φ_{x1} equal to $\Phi_0/2$ (or very close to it) transforms the potential into a symmetric (or nearly symmetric) double well. The flux Φ_c is changed between three different values: Φ_{c1} and Φ_{c2} define, respectively, high and intermediate amplitudes of the barrier between the two minima, whereas at $\Phi_{c3} = \Phi_{c2} + \Delta\Phi_c$ the barrier is removed completely and the potential turns into a single well. Varying the pulse amplitude $\Delta\Phi_c$ allows single wells of different curvature at the bottom to be created. The nominal rise and fall times of this pulse are $t_{r/f} = 0.6$ ns.

The flux sequence is repeated for 10^2–10^4 times in order to evaluate the probability $P_L = |\langle L|\Psi_{final}\rangle|^2$ of the left state occupation at the end of the manipulation. In figure 4(a), we show coherent oscillations between the states $|L\rangle$ and $|R\rangle$ which were obtained by changing the duration Δt of the manipulation pulse Φ_c. The oscillation frequency could be tuned between 6 and 21 GHz by changing the pulse amplitude $\Delta\Phi_c$. These oscillations persist when the potential is made slightly asymmetric by varying the value Φ_{x1}. As shown in figure 4(b), detuning from the symmetric potential by up to $\pm 2.9 m\Phi_0$ only slightly changes the amplitude and symmetry

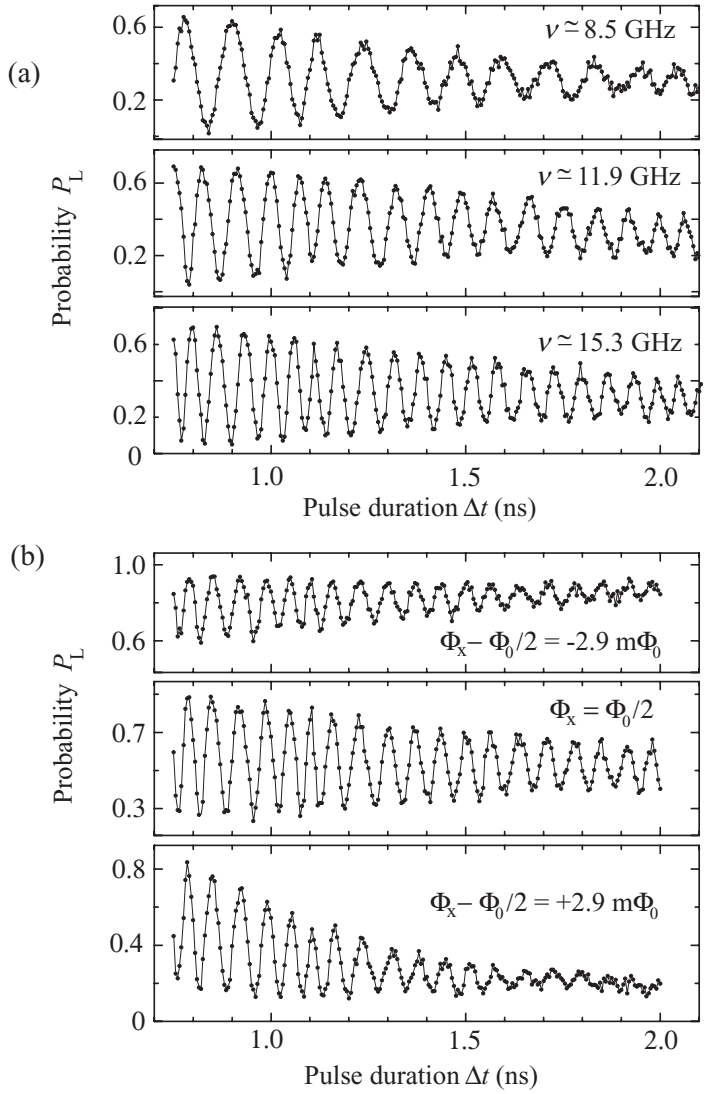

Figure 4. Dependence of the probability of measuring the state $|L\rangle$ on the pulse duration Δt for the qubit initially prepared in the $|L\rangle$ state, for (a) different pulse amplitudes $\Delta\Phi_c$, resulting in the indicated oscillation frequency, and (b) for different potential symmetry by detuning Φ_x from $\Phi_0/2$ by the indicated amount.

of the oscillations. When the qubit was initially prepared in state $|R\rangle$ instead of state $|L\rangle$, we observed similar oscillations as expected.

To understand the physical process behind the observed oscillations, let us discuss in detail what happens during the manipulation. Suppose the system is initially prepared in the left state $|L\rangle$ of a perfectly symmetric double well potential. During the Φ_c pulse, the potential has only one central minimum and can be approximated by an harmonic oscillator potential with frequency $\omega_0(\Phi_{c3}) \approx 1/\sqrt{2LC}\sqrt{1-\beta(\Phi_{c3})}$. The pulse transforms the initially prepared left state (that is a symmetric superposition of the two lowest energy eigenstates of the double well potential $|\tilde{0}\rangle$ and $|\tilde{1}\rangle$, i.e. $|L\rangle = (|\tilde{0}| + |\tilde{1}|)/\sqrt{2}$) into the superposition of the two lowest energy eigenstates $|0\rangle$ and $|1\rangle$ of the single-well potential. To achieve that, the pulse rise time needs

to be shorter than the relaxation time but, at the same time, long enough to avoid population of upper energy levels. During the plateau of the $\Delta\Phi_c$ pulse, the relative phase θ between the states $|0\rangle$ and $|1\rangle$ evolves in time at the Larmor frequency given by $\omega_0 = (E_1 - E_0)/\hbar$. At the end of the pulse the accumulated relative phase becomes $\theta = \omega_0 \Delta t$. Turning the system back into the double-well maps the phase to the two flux states $|L\rangle$ and $|R\rangle$. The final state after the flux pulse Φ_c is $|\Psi_{\text{final}}\rangle = \cos(\theta/2)\,|L\rangle + \mathrm{i}\sin(\theta/2)|R\rangle$. Note that in the more realistic case of a not perfectly symmetric double-well potential, the initial left state is no longer a symmetric superposition, but tends to either $|\tilde{0}\rangle$ or $|\tilde{1}\rangle$ due to the potential unbalancing. However, a pulse with a short rise time induces a nonadiabatic transition that populates mainly the two lowest energy eigenstates $|0\rangle$ and $|1\rangle$ in the single well potential. This condition can be met in a narrow region of the flux bias plane called the 'portal' [29]. This nonadiabatic transition also leads to the phase evolution process described above.

In order to verify the above interpretation, we numerically solved the time-dependent Schrödinger equation for this system. The simulation showed that, with our experimental parameters, the transition between the first two levels occurs as described, whereas the occupation of upper levels remains below a few percent.

The oscillation frequency ω_0 depends on the amplitude of the manipulation pulse $\Delta\Phi_c$ since it determines the shape of the single well potential and the energy level spacing $E_1 - E_0$. A pulse of larger amplitude $\Delta\Phi_c$ generates a deeper well having a larger level spacing, which leads to a larger oscillation frequency as shown in figure 4(a). In figure 5, we plot the energy spacing between the ground state and the three excited states (indicated as $(E_k - E_0)/h$ with $k = 1, 2, 3$) versus the flux $\Phi_{c3} = \Phi_{c2} + \Delta\Phi_c$ obtained from a numerical simulation of our system using the experimental parameters. In the same figure, we plot the measured oscillation frequencies for different values of Φ_c (open circles). Excellent agreement between simulation (solid line) and data strongly supports our interpretation. The fact that a small asymmetry in the potential does not change the oscillation frequency, as shown in figure 4(b), is consistent with the interpretation as the energy spacing $E_1 - E_0$ is only weakly affected by small variations of Φ_x. This provides protection against noise in the controlling flux Φ_x.

In order to independently measure the coherence times in our system, we operated the device as a conventional phase qubit [18, 30] which was possible due to its tunability. Here, the two logical qubit states were located in the shallow potential well of a strongly asymmetric double well potential. State transitions were induced by interaction with an applied resonant microwave field, allowing us to detect driven Rabi oscillations by changing the duration of the microwave pulse. The energy relaxation time T_1 was measured directly by observing the exponential decay of the excited state population probability after applying a microwave π-pulse. The measured value of $T_1 \approx 2\,\text{ns}$ is very close to the decay time of the coherent oscillations obtained by the flux pulse manipulation method reported above. Comparable coherence times are measured on similar devices fabricated using the same technology [31], suggesting that coherence is not limited by the novel manipulation procedure reported in this paper. We believe that the decay time of the reported high-frequency coherent oscillations can be increased by two orders of magnitude by reducing the area of the JJs and using an appropriate dielectric instead of SiO_2 as insulating material in the junction fabrication [30].

We note that a qubit manipulation without using microwaves has been reported previously by Koch *et al* [5], demonstrating Larmor oscillations in a flux qubit coupled to a harmonic oscillator. It should be emphasized that, in our case, the oscillator is not required, which simplifies the realization of the qubit circuit. Moreover, in contrast to [5], our approach provides

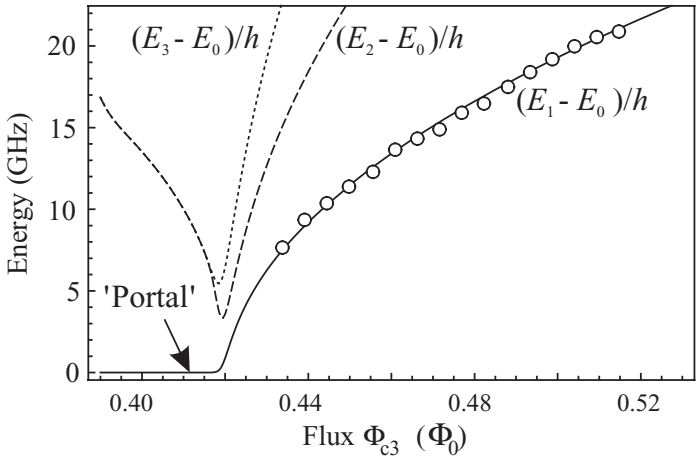

Figure 5. Calculated energy spacing of the first (solid line), second (dashed line) and third (dotted line) energy levels with respect to the ground state in the single well potential, plotted versus the control flux amplitude Φ_{c3}. Circles are the experimentally observed oscillation frequencies for the corresponding pulse amplitudes.

a *wide range tunability* of the frequency of coherent oscillations. This is important concerning the realization of a controllable coupling between qubits or quantum busses such as resonant cavities.

In conclusion, we presented the coherent manipulation of a flux qubit without using microwaves. The reported approach seems particularly promising for the realization of circuits with many qubits, and it appears to be well suited for integration with RSFQ control electronics [32, 33]. The benefits of the reported system are the possibility of *in situ* tuning the frequency of oscillations and their insensitivity to small changes in the potential symmetry. The high frequency of oscillations allows for very fast qubit gate operations, and the large energy gap between the qubit states during coherent evolution protects the system from thermal activation to upper energy states. Moreover, the oscillation frequency depends only weakly on the control pulse amplitude $\Delta\Phi_c$, in contrast to the exponential sensitivity of the oscillations in a double well potential [34], which makes the qubit manipulation more reliable.

Acknowledgments

This work was partially supported by the Deutsche Forschungsgemeinschaft (DFG), the CNR RSTL program and the EU projects RSFQubit and EuroSQIP.

References

[1] Nakamura Y, Pashkin Y A and Tsai J S 1999 Coherent control of macroscopic quantum states in a single-Cooper-pair box *Nature* **398** 786

[2] Martinis J M, Nam S, Aumentado J and Urbina C 2002 Rabi oscillations in a large Josephson-junction qubit *Phys. Rev. Lett.* **89** 117901

[3] Chiorescu I, Nakamura Y, Harmans C J P M and Mooij J E 2003 Coherent quantum dynamics of a superconducting flux qubit *Science* **299** 1869
[4] Vion D, Aassime A, Cottet A, Joyez P, Pothier H, Urbina C, Esteve D and Devoret M H 2002 Manipulating the quantum state of an electrical circuit *Science* **296** 886
[5] Koch R H, Keefe G A, Milliken F P, Rozen J R, Tsuei C C, Kirtley J R and DiVincenzo D P 2006 Experimental demonstration of an oscillator stabilized Josephson flux qubit *Phys. Rev. Lett.* **96** 127001
[6] Berkley A J, Xu H, Ramos R C, Gubrud M A, Strauch F W, Johnson P R, Anderson J R, Dragt A J, Lobb C J and Wellstood F C 2003 Entangled macroscopic quantum states in two superconducting qubits *Science* **300** 1548
[7] Pashkin Y A, Yamamoto T, Ostafiev O, Nakamura Y, Averin D V and Tsai J S 2003 Quantum oscillations in two coupled charge qubits *Nature* **421** 823
[8] Yamamoto T, Pashkin Yu A, Astafiev O, Nakamura Y and Tsai J S 2003 Demonstration of conditional gate operation using superconducting charge qubits *Nature* **425** 941
[9] Plantenberg J H, de Groot P C, Harmans C J P M and Mooij J E 2007 Demonstration of controlled-NOT quantum gates on a pair of superconducting quantum bits *Nature* **447** 836
[10] Sillanpää M A, Park J I and Simmonds R W 2007 Coherent quantum state storage and transfer between two phase qubits via a resonant cavity *Nature* **449** 438
[11] Majer J *et al* 2007 Coupling superconducting qubits via a cavity bus *Nature* **449** 443
[12] McDermott R, Simmonds R W, Steffen M, Cooper K B, Cicak K, Osborn K D, Oh S, Pappas D P and Martinis J M 2005 Simultaneous state measurement of coupled Josephson phase qubits *Science* **307** 1299
[13] Mooij J E, Orlando T P, Levitov L, Tian L, van der Wal C H and Lloyd S 1999 Josephson persistent-current qubit *Science* **285** 1036
[14] Lupaşcu A, Driessen E F C, Roschier L, Harmans C J P M and Mooij J E 2006 High-contrast dispersive readout of a superconducting flux qubit using a nonlinear resonator *Phys. Rev. Lett.* **96** 127003
[15] Saito S, Meno T, Ueda M, Tanaka H, Sembra K and Takayanagi H 2006 Parametric control of a superconducting flux qubit *Phys. Rev. Lett.* **96** 107001
[16] Steffen M, Martinis J M and Chuang I L 2003 Accurate control of Josephson phase qubits *Phys. Rev.* B **68** 224518
[17] Neeley M, Ansmann M, Bialczak R C, Hofheinz M, Katz N, Lucero E, O'Connell A, Wang H, Cleland A N and Marinis J M 2008 Process tomography of quantum memory in a Josephson-phase qubit coupled to a two-level state *Nat. Phys.* **4** 523
[18] Steffen M, Ansmann M, McDermott R, Katz N, Bialczak R C, Lucero E, Neeley M, Weig E M, Cleland A N and Martinis J M 2006 State tomography of capacitively shunted phase qubits with high fidelity *Phys. Rev. Lett.* **97** 050502
[19] Katz N *et al* 2006 Coherent state evolution in a superconducting qubit from partial-collapse measurement *Science* **312** 1498
[20] Claudon J, Balestro F, Hekking F W J and Buisson O 2004 Coherent oscillations in a superconducting multilevel quantum system *Phys. Rev. Lett.* **93** 187003
[21] Amin M H S 2006 Rabi oscillations in systems with small anharmonicity *J. Low Temp. Phys.* **32** 198
[22] Dutta S K *et al* 2008 Multilevel effects in the Rabi oscillations of a Josephson phase qubit *Phys. Rev.* B **78** 104510
[23] Schreier J A *et al* 2008 Suppressing charge noise decoherence in superconducting charge qubits *Phys. Rev.* B **77** 180502
[24] Wallraff A, Schuster D I, Blais A, Frunzio L, Majer J, Devoret M H, Girvin S M and Schoelkopf R J 2005 Approaching unit visibility for control of a superconducting qubit with dispersive readout *Phys. Rev. Lett.* **95** 060501
[25] Knill E 2005 Quantum computing with realistically noisy devices *Nature* **434** 39
[26] Cosmelli C, Carelli P, Castellano M G, Chiarello F, Leoni R and Torrioli G 2002 Measurements for an experiment of macroscopic quantum coherence with SQUIDs *Physica* C **372** 213

[27] Lukashenko A and Ustinov A V 2008 Improved powder filters for qubit measurements *Rev. Sci. Instrum.* **79** 014701
[28] Castellano M G *et al* 2007 Catastrophe observation in a Josephson-junction system *Phys. Rev. Lett.* **98** 177002
[29] Koch R H, Rozen J R, Keefe G A, Milliken F M, Tsuei C C, Kirtley J R and DiVincenzo D P 2005 Low-bandwidth control scheme for an oscillator-stabilized Josephson qubit *Phys. Rev.* B **72** 092512
[30] Martinis J M *et al* 2005 Decoherence in Josephson qubits from dielectric loss *Phys. Rev. Lett.* **95** 210503
[31] Lisenfeld J, Lukashenko A, Ansmann M, Martinis J M and Ustinov A V 2007 Temperature dependence of coherent oscillations in Josephson phase qubits *Phys. Rev. Lett.* **99** 170504
[32] Feldman M J and Bocko M F 2001 A realistic experiment to demonstrate macroscopic quantum coherence *Physica* C **350** 171
[33] Ohki T A, Wulf M and Feldman M J 2007 Low-Jc rapid single flux quantum (RSFQ) qubit control circuit *IEEE Trans. Appl. Supercond.* **17** 154
[34] Chiarello F 2007 Double SQUID tunable flux qubit manipulated by fast pulses: operation requirements, dissipation and decoherence *Eur. Phys. J.* B **55** 7